Mixed Ionic and Electronic Conducting Eutectogels for 3D-Printable Wearable Sensors and Bioelectrodes

Matías L. Picchio,* Antonela Gallastegui, Nerea Casado, Naroa Lopez-Larrea, Bastien Marchiori, Isabel del Agua, Miryam Criado-Gonzalez, Daniele Mantione, Roque J. Minari, and David Mecerreyes*

Eutectogels are a new class of soft ion conductive materials that are attracting attention as an alternative to conventional hydrogels and costly ionic liquid gels to build wearable sensors and bioelectrodes. Herein, the first example of mixed ionic and electronic conductive eutectogels showing high adhesion, flexibility, nonvolatility, and reversible low-temperature gel transition for 3D printing manufacturing is reporting. The eutectogels consist of choline chloride/glycerol deep eutectic solvent, poly(3,4-ethylenedioxythiophene): lignin sulfonate, and gelatin as the biocompatible polymer matrix. These soft materials are flexible and stretchable, show high ionic and electronic conductivities of 7.3 and 8.7 mS cm^{-1}, respectively, and have high adhesion energy. Due to this unique combination of properties, they could be applied as strain sensors to precisely detect physical movements. Furthermore, these soft mixed ionic electronic conductors possess excellent capacity as conformal electrodes to record epidermal physiological signals, such as electrocardiograms and electromyograms, over a long time.

1. Introduction

Soft and stretchable biocompatible conductors have attracted extensive research attention because of their great potentiality in the rapidly growing field of wearable digital devices.[1] For instance, organic mixed ionic-electronic conductors (OMIECs),

like poly(3,4-ethylenedioxythiophene):poly(styrene sulfonate) (PEDOT:PSS), stand out for this application due to their enhanced charge storage and coupled transport properties.[2–4] These functional materials are commonly used for recording physiological signals, assessing biochemical information, and electrical stimulation/modulation. Ionic-electronic conductive hydrogels are another important family of soft conductors that have been broadly explored in healthcare technologies due to their similarities to biological tissues and tunability in terms of electronic, mechanical, and chemical properties.[5] In particular, natural biopolymers-based hydrogels are attractive platforms for wearable devices as they combine inherent renewable, non-toxic features, biocompatibility, and biodegradability.[6,7] Several examples of natural biopolymers have been reported as promising building blocks in stretchable devices, including cellulose,[8–10] chitosan,[11–13] alginate,[14–16] silk fibroin,[17,18] and gelatin.[19–21]

Unfortunately, these conductive hydrogels fail in long-lasting signals recording due to the continuous water evaporation in open-air sensors and bioelectrodes. At this point, ionic liquid

M. L. Picchio, R. J. Minari
Instituto de Desarrollo Tecnológico para la Industria Química (INTEC)
CONICET
Güemes 3450, Santa Fe 3000, Argentina
E-mail: mlpicchio@santafe-conicet.gov.ar

M. L. Picchio
Departamento de Química Orgánica
Facultad de Ciencias Químicas (Universidad Nacional de Córdoba)
IPQA–CONICET
Haya de la Torre y Medina Allende
Córdoba 5000, Argentina

The ORCID identification number(s) for the author(s) of this article can be found under https://doi.org/10.1002/admt.202101680.

A. Gallastegui, N. Casado, N. Lopez-Larrea, M. Criado-Gonzalez, D. Mecerreyes
POLYMAT University of the Basque Country UPV/EHU
Joxe Mari Korta Center
Avda. Tolosa 72, Donostia-San Sebastián 20018, Spain
E-mail: david.mecerreyes@ehu.es

B. Marchiori, I. del Agua
Panaxium SAS
Aix-en-Provence 13100, France

D. Mantione
POLYKEY POLYMERS s.l.
Joxe Mari Korta Center
Avda. Tolosa 72, Donostia-San Sebastian 20018, Spain

D. Mecerreyes
Ikerbasque
Basque Foundation for Science
Bilbao 48013, Spain

**ADVANCED
SCIENCE NEWS**
www.advancedsciencenews.com

**ADVANCED
MATERIALS
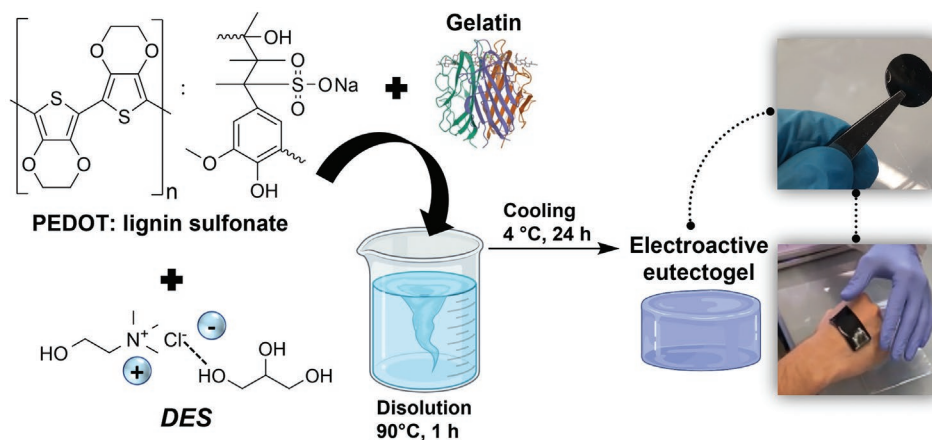TECHNOLOGIES**
www.advmattechnol.de

Figure 1. Schematic illustration of the construction of the electroactive gelatin-based eutectogels.

gels or iongels with characteristic low vapor pressure and high ionic conductivity have stepped into the spotlight in the last five years.[22–26] As a representative example, Luque et al. have recently reported 3D-printable poly(vinyl alcohol)-based iongels using cholinium-derived ionic liquids (ILs) and polyphenols as dynamic crosslinkers for long-term cutaneous electrophysiological recordings.[27] However, ILs are expensive, and their green character has often been questioned due to their poor biocompatibility and biodegradability.[28]

Under this scenario, eutectogels, an emerging class of ionic materials that have just been developed very recently, offer unique opportunities for creating novel flexible bioelectronics.[29,30] In these soft conductors, the liquid phase is a deep eutectic solvent (DES), sharing many of the features of the ILs like high thermal stability and ionic conductivity, but benefiting from easy preparation, low cost, and noncytotoxicity.[31–33] Up to now, only a few examples of purely ionic conductive eutectogels for bioelectronics have been reported.[34–37] Very recently, Ouyang et al. prepared waterborne polyurethane-based eutectogels using choline chloride (ChCl)/glycerol (Gly) DES and tannic acid as a crosslinker for self-adhesive bioelectrodes. These soft ionic conductors showed good extensibility of 178% and ionic conductivity of 0.22 mS cm^{-1}.[37]

In this work, we develop biocompatible soft conductors composed of ChCl/Gly, PEDOT: lignin sulfonate, and gelatin as the first example of mixed ionic and electronic eutectogels for flexible electronics. These gels combine properties like high adhesion, stretchability, good electronic and ionic conductivity, and thermoreversible gel transition, endowing them with 3D printing and remolding abilities. Altogether, these features render the eutectogels promising platforms as conformal movement sensors and electrodes for long-term monitoring of body signals through electrocardiogram (ECG) and electromyogram (EMG).

2. Results and Discussion

As schematized in **Figure 1**, the eutectogels were synthesized via a three-step process, including i) the dispersion of PEDOT: lignin sulfonate (2% w/v) powder into the DES, ii) mixing gelatin (20% w/v) at 90 °C into the PEDOT: lignin sulfonate/DES to obtain unentangled gelatin random coils, and iii) pouring the warm precursor solution into a mold and cooling it overnight at 4 °C to promote gelatin triple helix formation based on hydrogen bonds.[38] First, we screened different gelatin concentrations to prepare purely ionic eutectogels, 10, 20, and 30% w/v. Then, a 20% w/v concentration was selected to meet an optimal balance between solution viscosity and gel elasticity (see viscoelastic properties in Figure S1A of the Supporting Information). On the other hand, lignin sulfonate was chosen for PEDOT stabilization as this plant-derived polyphenol has good biocompatibility and may also contribute to gel adhesion.[39] Thus, we explored different PEDOT: lignin sulfonate weight ratios (60:40, 70:30, 80:20, and 90:10) to modulate the gels' electronic conductivity and properties. According to the PEDOT: lignin sulfonate ratio used, the obtained eutectogels were coded as eGel-60, eGel-70, eGel-80, eGel-90, and eGel-0 for the purely ionic eutectogel.

ATR-FTIR spectroscopy was employed to analyze the nature of the interactions between the eutectogel components. As shown in **Figure 2**A, the characteristic signals of gelatin and the DES at 1627 cm^{-1} (Amide I, C=O ν), 1522 cm^{-1} (Amide II, N–H δ) and 1035 cm^{-1} (C–O ν) showed a hypsochromic shift, after gel formation, to 1649 cm^{-1}, 1552 cm^{-1}, and 1040 cm^{-1}, respectively. Besides, a band broadening was observed in the region 3200–3500 cm^{-1}, corresponding to Amide A (N–H ν) and O–H ν. These results suggest the formation of strong hydrogen bonds between the DES and the gelatin scaffold, which are not affected by the PEDOT: lignin sulfonate addition (2% w/v), as observed in FTIR spectra of Figure S1B of the Supporting Information.

Indeed, these excellent interactions in the eutectogel matrix provide the materials with high thermal stability. As shown in the thermograms of Figure 2B, all the samples presented a similar degradation profile with an initial weight loss of around 8% at 100 °C, probably associated with water evaporation as the eutectogel components are highly hygroscopic. Regardless of the PEDOT: lignin sulfonate ratio, the main decomposition process starts at around 200 °C, demonstrating a wide window for thermal processing.
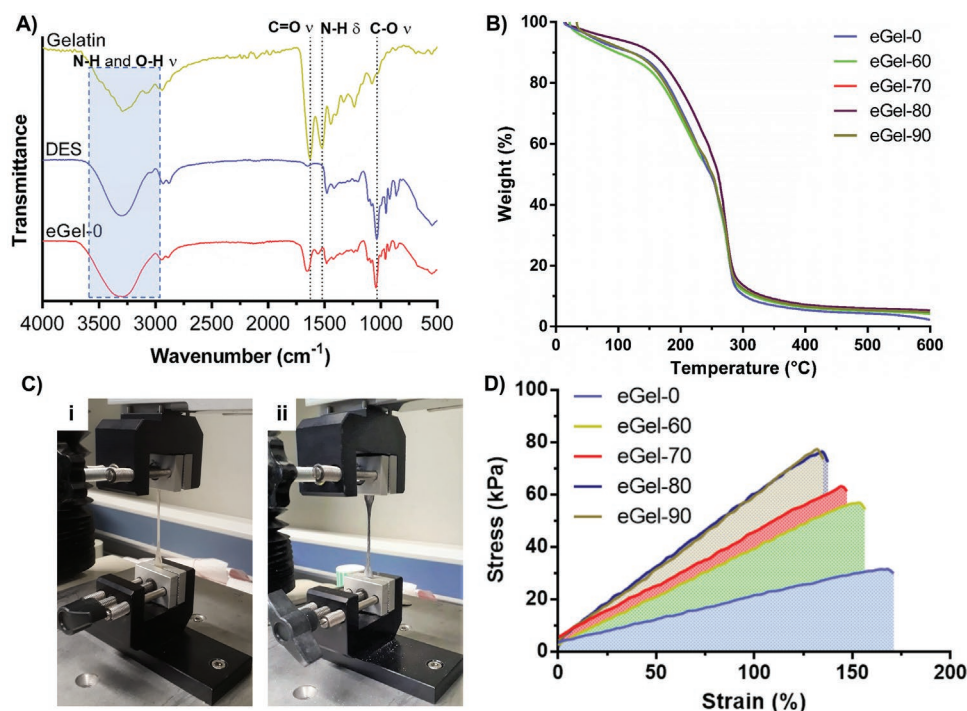
2101680 (2 of 8)

ADVANCED
SCIENCE NEWS
www.advancedsciencenews.com

ADVANCED
MATERIALS
TECHNOLOGIES
www.advmattechnol.de

Figure 2. A) FTIR spectra of gelatin, ChCl/Gly DES, and eGel-0 eutectogel. B) Degradation profile of the as-prepared eutectogels. C) Images of the tensile test of eGel-0 (i) and eGel-90 (ii). D) Stress versus strain curves for the electroactive materials.

Dynamic hydrogen bonding also endows eutectogels with good stretchability and strength, as shown in Figure 2C,D and Video S1 of the Supporting Information. We found that when increasing the PEDOT: lignin sulfonate ratio, the eutectogels breaking strength increased, but their extensibility decreased, suggesting that the conducting polymer acts as a reinforcer of the biopolymer matrix (Figure 2D). For instance, the fracture strain varied from 165% to 130%, while the breaking strength increased from 32 to 78 kPa for eGel-0 and eGel-90, respectively. Interestingly, the eutectogels showed a linear elastic behavior until the sample fracture, with Young's moduli ranging 18–50 kPa and resilience values of around 50 kJ m^{-3} (Figure S2 of the Supporting Information).

Next, we investigated the viscoelastic properties of the eutectogels by small-amplitude oscillatory shear (SAOS). As an example, the amplitude and frequency sweeps of eGel-90 are displayed in **Figure 3**A,B. The gels showed elastic moduli (G') in the order of 10 kPa and large linear viscoelastic ranges (LVR) higher than 25% (see Figure S3 of the Supporting Information), in good agreement with the extended proportional limit observed in the tensile tests. In addition, frequency sweeps revealed that these dynamic materials are stable gels in the standard frequency range of 0.1–100 rad s^{-1}, showing no crossover point between G' and viscous modulus (G'') (Figure S4 of the Supporting Information). At high frequency (>30 rad s^{-1}), all the samples presented an increase in the dynamic moduli, likely due to long entangled gelatin chains with long relaxation times, acting as crosslinking points.[40]

On the other hand, owing to the dynamic nature of the electroactive eutectogels, they show thermoreversible gel-sol transition, which is a valuable feature for 3D printing applications.

Therefore, we investigated the thermal behavior of these soft conductors by differential scanning calorimetry (DSC) and dynamic mechanical thermal analysis (DMTA).

From the DSC scannings of Figure 3C, it can be observed that the gels presented a glass transition occurring almost simultaneously with their gel-sol transition temperature at around 55–60 °C. These results are supported by DMTA, where all the gels showed a clear crossover point ($G' = G''$) at around 55 °C, indicating this gel to liquid phase transition (Figure 3D and Figure S5 of the Supporting Information). It is worth mentioning that unlike previously reported PEDOT:PSS printable inks,[41] the eutectogels rheological behavior was not significantly influenced by the conducting polymer concentration mainly because the gelatin matrix dominated the viscoelastic properties of these materials.

Moreover, although the eutectogels presented a predominant solid-like behavior ($G' > G''$) below ≈55 °C, they can be easily extruded at mild temperatures and low pressures. We found an optimal extrusion temperature close to the onset of the G' decay. Otherwise, lower or higher temperatures led to material clogging or lateral spreading upon extrusion, respectively. Indeed, Figure 3E shows that eGel-90 could be perfectly shaped at 42 °C with a 3D printer in different patterns.

At this point, we studied the electronic properties of these materials: the electronic conductivity given by the semiconducting polymer and the ionic conductivity given by the DES. First, we evaluated their electronic conductivities (σ_e) by 4-point probe measurements. The values of σ_e ranged between 2.2 and 8.7 mS cm^{-1}, and as expected, the higher the PEDOT:lignin sulfonate ratio, the higher the eutectogels' conductivity (**Figure 4**A). Thus, eGel-90 was chosen to perform further cyclic

**ADVANCED
SCIENCE NEWS**

www.advancedsciencenews.com

**ADVANCED
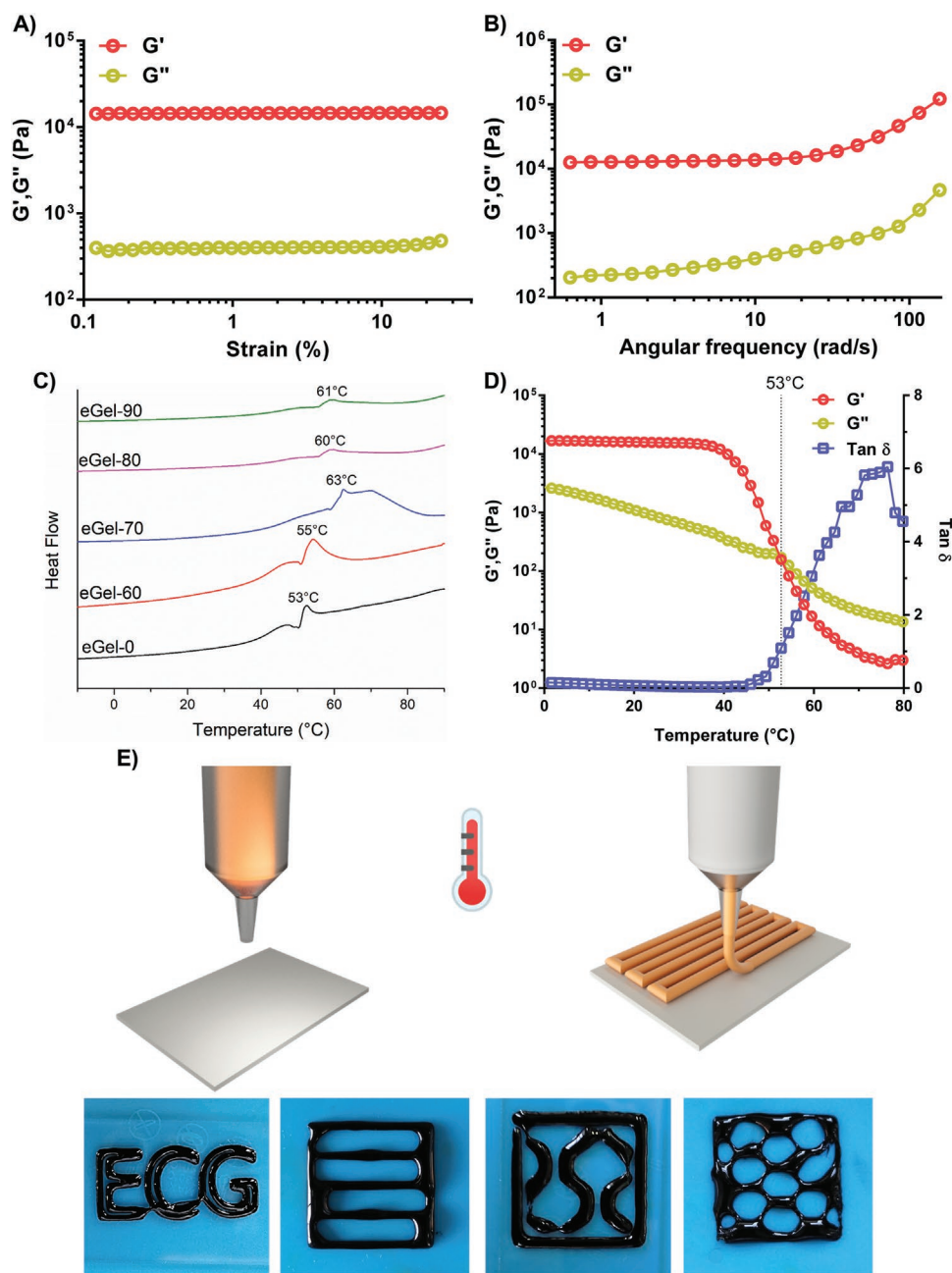MATERIALS
TECHNOLOGIES**

www.advmattechnol.de

Figure 3. Viscoelastic behavior of eGel-90 obtained by A) amplitude and B) frequency sweeps. C) DSC curves of electroactive eutectogels with different PEDOT content. D) Evolution of G', G'' and Tan δ versus temperature for eGel-90. E) 3D printing of eGel-90 in different patterns by hot extrusion at mild temperature (42 °C). Extrusion was performed at a pressure of 2 bar and a speed of 10 mm s^{-1}.

voltammetry experiments aiming to confirm its electroactivity. The cyclic voltammograms at scan rates from 20 to 150 mV s^{-1} in 0.1 M HClO$_4$ solution are shown in Figure 4B. We observed broad anodic and cathodic peaks, typical of PEDOT and similar to previous results.[42,43] In addition, the anodic and cathodic peak currents were proportional to the scan rate (see Figure S6 of the Supporting Information), indicating that the redox process is not controlled by diffusion and demonstrating the electroactivity of the eutectogels.

Then, we analyzed the gels' ionic conductivity (σ_i) by electrochemical impedance spectroscopy from 30 to 90 °C, as

shown in Figure 4C. The results showed ionic conductivities in the order of 10^{-2} S cm^{-1}, and we observed the typical linear dependence of σ_i versus temperature due to the increase in carrier mobility. As expected, the immobilization of the DES in the gelatin matrix decreased its conductivity, but curiously, σ_i increased with the PEDOT:LS ratio, obtaining a maximum value of 5.5 mS cm^{-1} for eGel-90 at 30 °C. This fact shows the positive contribution of oxidized PEDOT chains in the average ionic conductivity.[44] Figure 4D shows a LED-light circuit in ON state, built with eGel-90 as proof of the excellent conductivity of this eutectogel.
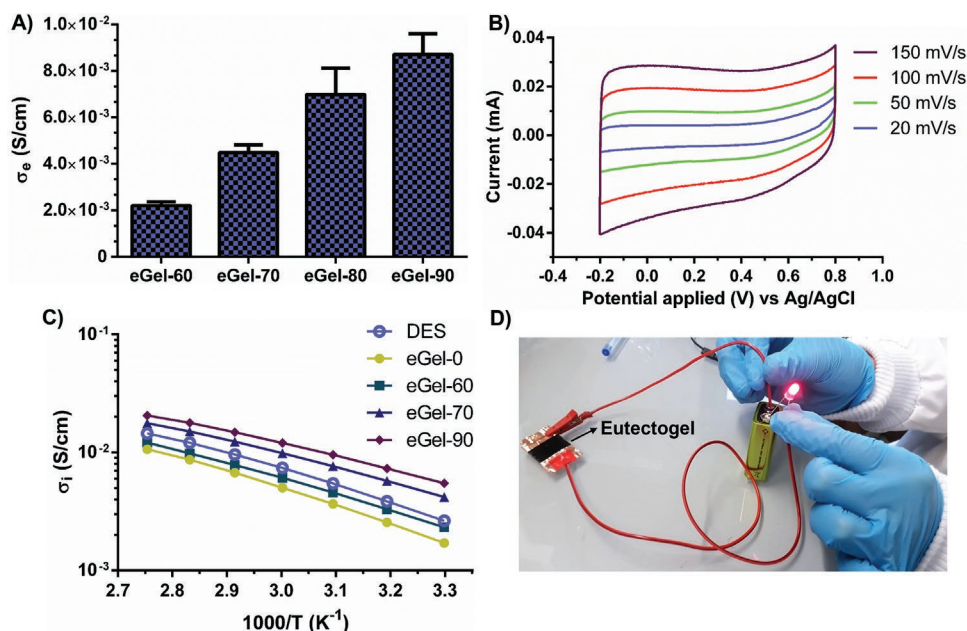
**ADVANCED
SCIENCE NEWS**

www.advancedsciencenews.com

**ADVANCED
MATERIALS
TECHNOLOGIES**

www.advmattechnol.de

Figure 4. A) Electronic conductivity of the as-prepared eutectogels with varied PEDOT: LS ratio. B) Cyclic voltammetry of eGel-90 at scanning rates of 20, 50, 100, and 150 mV s^{-1}. C) Ionic conductivity versus temperature for different eutectogels, and DES was included for comparison purposes. D) Photograph of the ON state of a LED-light circuit built with eGel-90.
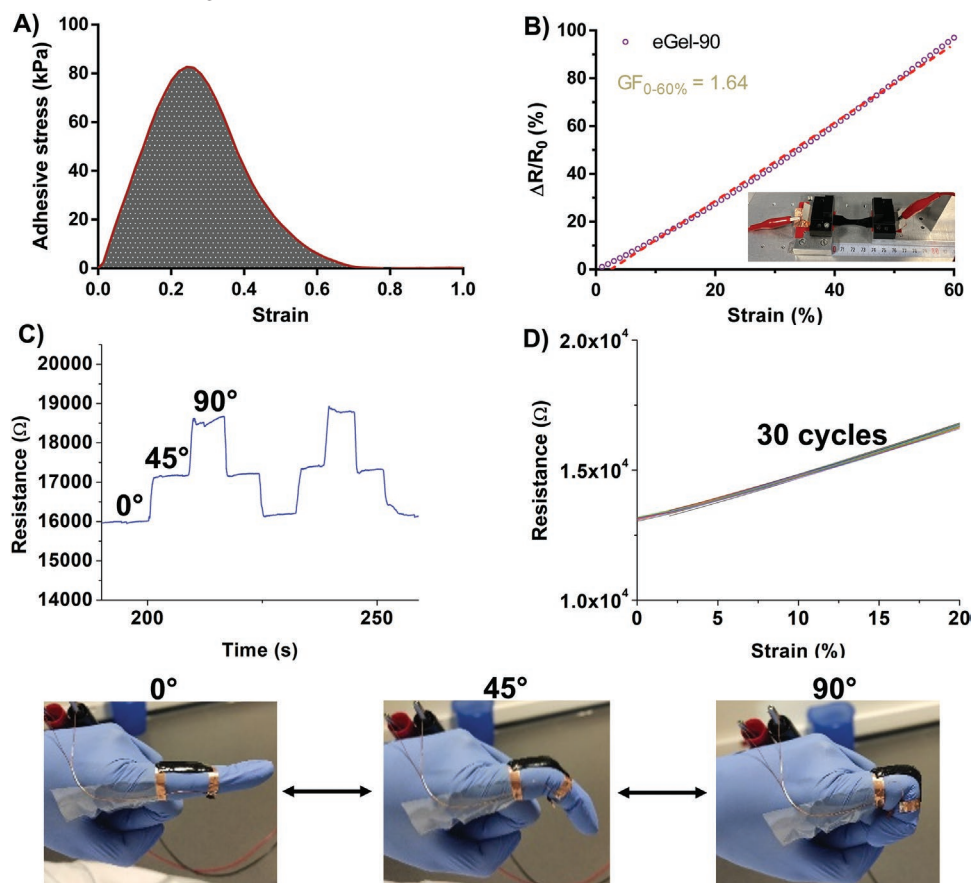

Figure 5. A) Adhesive stress versus strain curve for eGel-90. B) Variation of $\Delta R/R_0$ of eGel-90 eutectogel with the strain. Inset: stretching of eGel-90 during resistance measurements. C) Resistance responses of the eGel-90 sensor when the index finger bends at different degrees: 0°-45°-90°. D) Resistance versus strain relationship during 30 consecutive stretching–releasing cycles at 20% of strain for eGel-90. Bottom: images of the index finger bending at different degrees.

2101680 (5 of 8)

ADVANCED
SCIENCE NEWS

www.advancedsciencenews.com

ADVANCED
MATERIALS
TECHNOLOGIES

www.advmattechnol.de

Finally, since the highest combined ionic and electronic conductivity of eGel-90, we chose this material to evaluate its potential use as a soft sensor and electrode for bioelectronics. An exciting feature of these materials is their excellent adhesion to the skin (see Video S2 in the Supporting Information), which favors an intimate contact, essential for conformal wearable devices. For instance, according to probe tack measurements, eGel-90 possesses an adhesion strength of 80 kPa and adhesion energy (proportional to the area under stress vs strain curve) of 33 J m^{-2} (**Figure 5**A), much higher than those for recently reported hydrogels with similar properties.[45,46] Then, eGel-90 was applied as a strain sensor to detect physical movements. The sensor sensitivity is determined by the resistance variation percentage, $\Delta R/R_0$, where R_0 and R are the resistances of the eutectogel at rest and under strain. $\Delta R/R_0$ shows a linear relationship with the strain in the range of 0–60%, and the gauge factor (GF) is 1.64 (Figure 5B). eGel-90 sensor stuck on the surface of an index finger shows smooth signals with low noise, and the signals are sensitive to the bending angle of the finger (Figure 5C and Figure S7A and Video S3, Supporting Information), displaying good reproducibility during different bending cycles. Since the excellent stretchability and large elastic limit of the eutectogel, the sensor maintains a linear dependency with the strain even after 30 or 20 stretching–releasing cycles with a maximum strain of 20% or 30%, without compromising its sensitivity (see Figure 5D and Figure S7B, Supporting Information).

In addition, we also investigated the performance of eGel-90 as a cutaneous bioelectrode for ECG and EMG recording. The adhesive eutectogel and an Ag/AgCl gel medical electrode used as control were attached to the wrist of a female volunteer to register ECG signals (**Figure 6**A). In the ECG displayed in Figure 6B, PQRST waveforms were well detected, and the eutectogel presented comparable signals to the commercial control. Physiological signals provide valuable information for diagnosis and rehabilitation, and long-term biopotential monitoring is often demanded. Overtime ECG recordings using Ag/AgCl medical electrodes are impossible to obtain as they dry in a few hours. However, because of its nonvolatile nature, eGel-90 can reproduce high-quality ECG signals even
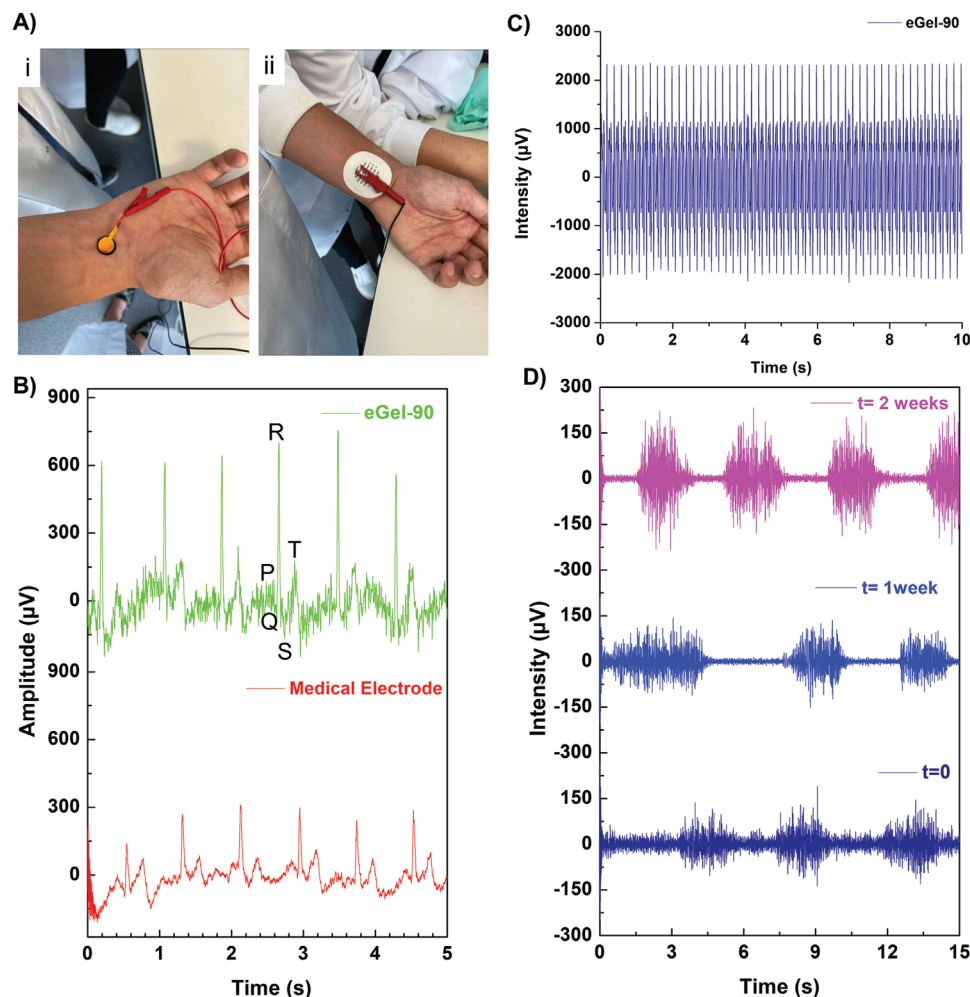

Figure 6. A) Images of eGel-90 (left) and Ag/AgCl medical electrode (right) attached to the wrist of a female volunteer. B) Comparison of the ECG signals using the adhesive eGel-90 electrode and a commercial medical electrode. C) EMG response of eGel-90 electrode after thigh stimulation of a female volunteer. D) Evolution over time of the EMG signals generated by thigh contraction/relaxation.

after two weeks, with stable outputs maintaining shape and intensity (see Figure S8, Supporting Information). Besides, this soft material can record EMG signals generated by thigh electrostimulation (see Figure 6C) and monitor muscle contraction/relaxation, obtaining excellent signal quality for at least 2 weeks, as shown in Figure 6D. These results reveal the ability of the eutectogel for long-lasting physiological recording.

3. Conclusions

This article presents a new type of eutectogel that combines the properties of a flexible biopolymer (gelatin), a conducting polymer (PEDOT:lignin sulfonate), and a deep eutectic solvent (ChCl/Gly), which acted as a dynamic crosslinker by hydrogen bonding interactions. These materials serve as a proof of concept and the first example of mixed ionic-electronic conducting eutectogels. The eutectogel formulation showing the highest ionic conductivity was found to be the one containing 90:10 PEDOT:lignin sulfonate weight ratio due to the contribution of the conducting polymer chains in the overall gel conductivity. Collectively, these soft conductors gather adhesion properties, elasticity, electroactivity, 3D-printing ability, and the ionic conductivity of the deep eutectic solvent together with their biocompatibility and negligible vapor pressure. This unique combination of properties turns these eutectogels into excellent platforms for wearable devices as soft sensors and conformal bioelectrodes. It is anticipated that a similar synthetic approach could be applied to other conducting polymers and deep eutectic solvents combinations, opening new directions for designing innovative low-cost soft bioelectronics.

Supporting Information

Supporting Information is available from the Wiley Online Library or from the author.

Conflict of Interest

The authors declare no conflict of interest.

Data Availability Statement

The data that support the findings of this study are available from the corresponding author upon reasonable request.

[1] H. Yuk, B. Lu, X. Zhao, *Chem. Soc. Rev.* **2019**, *48*, 1642.
[2] B. D. Paulsen, K. Tybrandt, E. Stavrinidou, J. Rivnay, *Nat. Mater.* **2020**, *19*, 13.
[3] D. Ohayon, S. Inal, *Adv. Mater.* **2020**, *32*, 2001439.
[4] M. ElMahmoudy, S. Inal, A. Charrier, I. Uguz, G. G. Malliaras, S. Sanaur, *Macromol. Mater. Eng.* **2017**, *302*, 1600497.
[5] F. Fu, J. Wang, H. Zeng, J. Yu, *ACS Mater. Lett.* **2020**, *2*, 1287.
[6] C. Cui, Q. Fu, L. Meng, S. Hao, R. Dai, J. Yang, *ACS Appl. Bio Mater.* **2021**, *4*, 85.
[7] C. Wang, T. Yokota, T. Someya, *Chem. Rev.* **2021**, *121*, 2109.
[8] R. Tong, G. Chen, D. Pan, H. Qi, R. Li, J. Tian, F. Lu, M. He, *Biomacromolecules* **2019**, *20*, 2096.
[9] X. F. Zhang, X. Ma, T. Hou, K. Guo, J. Yin, Z. Wang, L. Shu, M. He, J. Yao, *Angew. Chem., Int. Ed.* **2019**, *58*, 7366.
[10] Y. Wang, L. Zhang, A. Lu, *ACS Appl. Mater. Interfaces* **2019**, *11*, 41710.
[11] X. Wei, K. Ma, Y. Cheng, L. Sun, D. Chen, X. Zhao, H. Lu, B. Song, K. Yang, P. Jia, *ACS Appl. Polym. Mater.* **2020**, *2*, 2541.
[12] S. Xia, S. Song, F. Jia, G. Gao, *J. Mater. Chem. B* **2019**, *7*, 4638.
[13] C. Cui, C. Shao, L. Meng, J. Yang, *ACS Appl. Mater. Interfaces* **2019**, *11*, 39228.
[14] X. Zhang, N. Sheng, L. Wang, Y. Tan, C. Liu, Y. Xia, Z. Nie, K. Sui, *Mater. Horiz.* **2019**, *6*, 326.
[15] S. Yang, L. Jang, S. Kim, J. Yang, K. Yang, S. W. Cho, J. Y. Lee, *Macromol. Biosci.* **2016**, *16*, 1653.
[16] H. Liu, M. Li, C. Ouyang, T. J. Lu, F. Li, F. Xu, *Small* **2018**, *14*, 1801711.
[17] J. Yang, J. Luo, H. Liu, L. Shi, K. Welch, Z. Wang, M. Strømme, *Ind. Eng. Chem. Res.* **2020**, *59*, 9310.
[18] M. Yao, D. Su, W. Wang, X. Chen, Z. Shao, *ACS Appl. Mater. Interfaces* **2018**, *10*, 38466.
[19] C. Liu, H. J. Zhang, X. You, K. Cui, X. Wang, *Adv. Electron. Mater.* **2020**, *6*, 2000040.
[20] Z. Qin, X. Sun, H. Zhang, Q. Yu, X. Wang, S. He, F. Yao, J. Li, *J. Mater. Chem. A* **2020**, *8*, 4447.
[21] H. Chen, X. Ren, G. Gao, *ACS Appl. Mater. Interfaces* **2019**, *11*, 28336.
[22] P. Leleux, C. Johnson, X. Strakosas, J. Rivnay, T. Hervé, R. M. Owens, G. G. Malliaras, *Adv. Healthcare Mater.* **2014**, *3*, 1377.
[23] M. Isik, T. Lonjaret, H. Sardon, R. Marcilla, T. Herve, G. G. Malliaras, E. Ismailova, D. Mecerreyes, *J. Mater. Chem. C* **2015**, *3*, 8942.
[24] L. C. Tomé, L. Porcarelli, J. E. Bara, M. Forsyth, D. Mecerreyes, *Mater. Horiz.* **2021**, *8*, 3239.
[25] H. Dinh Xuan, B. Timothy, H. Y. Park, T. N. Lam, D. Kim, Y. Go, J. Kim, Y. Lee, S. Il Ahn, S. H. Jin, J. Yoon, *Adv. Mater.* **2021**, *33*, 2008849.
[26] L. Xu, Z. Huang, Z. Deng, Z. Du, T. L. Sun, Z. H. Guo, K. Yue, *Adv. Mater.* **2021**, *33*, 2105306.
[27] G. C. Luque, M. L. Picchio, A. P. S. Martins, A. Dominguez-Alfaro, N. Ramos, I. del Agua, B. Marchiori, D. Mecerreyes, R. J. Minari, L. C. Tomé, *Adv. Electron. Mater.* **2021**, *7*, 2100178.
[28] A. Paiva, R. Craveiro, I. Aroso, M. Martins, R. L. Reis, A. R. C. Duarte, *ACS Sustainable Chem. Eng.* **2014**, *2*, 1063.
[29] L. C. Tomé, D. Mecerreyes, *J. Phys. Chem. B* **2020**, *124*, 8465.
[30] J. D. Mota-Morales, E. Morales-Narváez, *Matter* **2021**, *4*, 2141.

[31] B. B. Hansen, S. Spittle, B. Chen, D. Poe, Y. Zhang, J. M. Klein, A. Horton, L. Adhikari, T. Zelovich, B. W. Doherty, B. Gurkan, E. J. Maginn, A. Ragauskas, M. Dadmun, T. A. Zawodzinski, G. A. Baker, M. E. Tuckerman, R. F. Savinell, J. R. Sangoro, *Chem. Rev.* **2021**, *121*, 1232.

[32] B. E. Gurkan, E. J. Maginn, E. B. Pentzer, *J. Phys. Chem. B* **2020**, *124*, 11313.

[33] C. Zhu, D. Huo, Q. Chen, J. Xue, S. Shen, Y. Xia, *Adv. Mater.* **2017**, *29*, 1703702.

[34] J. Wang, Y. Deng, Z. Ma, Y. Wang, S. Zhang, L. Yan, *Green Chem.* **2021**, *23*, 5120.

[35] S. Hong, Y. Yuan, C. Liu, W. Chen, L. Chen, H. Lian, H. Liimatainen, *J. Mater. Chem. C* **2020**, *8*, 550.

[36] H. Qin, R. E. Owyeung, S. R. Sonkusale, M. J. Panzer, *J. Mater. Chem. C* **2019**, *7*, 601.

[37] S. Wang, H. Cheng, B. Yao, H. He, L. Zhang, S. Yue, Z. Wang, J. Ouyang, *ACS Appl. Mater. Interfaces* **2021**, *13*, 20735.

[38] Z. Qin, D. Dong, M. Yao, Q. Yu, X. Sun, Q. Guo, H. Zhang, F. Yao, J. Li, *ACS Appl. Mater. Interfaces* **2019**, *11*, 21184.

[39] S. Sugiarto, Y. Leow, C. L. Tan, G. Wang, D. Kai, *Bioact. Mater.* **2021**, *8*, 71.

[40] M. J. Moura, M. M. Figueiredo, M. H. Gil, *Biomacromolecules* **2007**, *8*, 3823.

[41] H. Yuk, B. Lu, S. Lin, K. Qu, J. Xu, J. Luo, X. Zhao, *Nat. Commun.* **2020**, *11*, 1604.

[42] N. Casado, M. Hilder, C. Pozo-Gonzalo, M. Forsyth, D. Mecerreyes, *ChemSusChem* **2017**, *10*, 1783.

[43] F. N. Ajjan, N. Casado, T. Rębiś, A. Elfwing, N. Solin, D. Mecerreyes, O. Inganäs, *J. Mater. Chem. A* **2016**, *4*, 1838.

[44] I. Del Agua, D. Mantione, N. Casado, A. Sanchez-Sanchez, G. G. Malliaras, D. Mecerreyes, *ACS Macro Lett.* **2017**, *6*, 473.

[45] L. Han, L. Yan, M. Wang, K. Wang, L. Fang, J. Zhou, J. Fang, F. Ren, X. Lu, *Chem. Mater.* **2018**, *30*, 5561.

[46] Y. Zhao, Z. Li, S. Song, K. Yang, H. Liu, Z. Yang, J. Wang, B. Yang, Q. Lin, *Adv. Funct. Mater.* **2019**, *29*, 1901474.